Conformational Change Induced by ATP Binding in the Multidrug ATP-Binding Cassette Transporter BmrA†

Cédric Orelle,‡,§ Francesca Gubellini,|| Anne Durand,⊥ Sergio Marco,▽ Daniel Lévy,|| Philippe Gros,£ Attilio Di Pietro,‡ and Jean-Michel Jault*,⊥

Institut de Biologie et Chimie des Protéines, UMR 5086 CNRS−Université de Lyon 1 and IFR 128 BioSciences Gerland-Lyon Sud, 7 passage du Vercors, 69367 Lyon, France, Institut Curie, UMR-CNRS 168, 11 rue Pierre et Marie Curie, 75231 Paris, France, Institut de Biologie Structurale, UMR 5075 Université Joseph Fourier/CEA/CNRS, 41 rue Jules Horowitz, 38027 Grenoble cedex 1, France, Institut Curie, Unité INSERM 759, Centre Universitaire, Bât. 112, Orsay, France, and Department of Biochemistry, McGill University, Montreal, Québec H3G 1Y6, Canada

Received November 21, 2007

ABSTRACT: ATP-binding cassette (ABC) transporters are involved in the transport of a wide variety of substrates, and ATP-driven dimerization of their nucleotide binding domains (NBDs) has been suggested to be one of the most energetic steps of their catalytic cycle. Taking advantage of the propensity of BmrA, a bacterial multidrug resistance ABC transporter, to form stable, highly ordered ring-shaped structures [Chami et al. (2002) *J. Mol. Biol. 315*, 1075−1085], we show here that addition of ATP in the presence of Mg^{2+} prevented ring formation or destroyed the previously formed rings. To pinpoint the catalytic step responsible for such an effect, two classes of hydrolysis-deficient mutants were further studied. In contrast to hydrolytically inactive glutamate mutants that behaved essentially as the wild-type, lysine Walker A mutants formed ring-shaped structures even in the presence of ATP-Mg. Although the latter mutants still bound ATP-Mg, and even slowly hydrolyzed it for the K380R mutant, they were most likely unable to undergo a proper NBD dimerization upon ATP-Mg addition. The ATP-driven dimerization step, which was still permitted in glutamate mutants and led to a stable conformation suitable to monitor the growth of 2D crystals, appeared therefore responsible for destabilization of the BmrA ring structures. Our results provide direct visual evidence that the ATP-induced NBD dimerization triggers a conformational change large enough in BmrA to destabilize the rings, which is consistent with the assumption that this step might constitute the "power stroke" for ABC transporters.

Cellular export or import of a multitude of substrates including ions, sugars, lipids, amino acids, or drugs is a vital process governed by different classes of transporters (*1*). In many microbial genomes, the largest gene superfamily encodes transporters powered by ATP hydrolysis: the ATP-binding cassette (ABC)[1] transporters (*2*, *3*). Prominent members of this family also exist in eukaryotes whose dysfunction or exacerbated function plays a causative role in human pathologies such as cystic fibrosis, adrenoleukodystrophy, and multidrug resistance of cancer cells (*4*). The basic architecture of ABC transporters includes four core domains: two transmembrane domains that harbor the substrate-binding site(s) and two nucleotide-binding domains (NBDs) that bind and hydrolyze ATP. These domains are either expressed as single polypeptides or fused into different combinations to form three, two, or even one multidomain polypeptide(s). The NBDs contain three characteristic motifs: the Walker A and B motifs, found in many different ATPases, and a signature motif specific for the ABC family (*5*). Three-dimensional (3D) structures have been determined for several isolated NBDs, which all share the same overall topology (*6*). Although the molecular basis that drives the interaction of two NBDs within an ABC transporter had been a controversial issue, it is now accepted that the transporter is capable of hydrolyzing ATP in a transient conformation, with its two ATP-binding sites being properly oriented at the interface of the two NBDs: one contributes both the Walker A and B motifs, while the other interacts with ATP through its ABC signature motif (*7*, *8*). Such a closed conformation has been observed in the dimeric structure of NBDs from either inactive mutants (*9*−*11*) or the *Escherichia coli* MalK subunit of the maltose importer (*12*), both in the presence of ATP, and also in the vitamin B12 whole transporter BtuCD (*13*). Two additional "empty" structures

† This work was supported by CNRS Grant PGP 2002 (to A.D.P.), a CNRS Young Investigator ATIP Program to J.-M.J., and a grant (ANR-06-Blan-0420) from the Agence Nationale de la Recherche to A.D.P., D.L., and J.-M.J. C.O. was the recipient of fellowships from the Ministère de la Recherche, Fondation pour la Recherche Médicale, and Région Rhône-Alpes, EURODOC program. F.G. was the recipient of the Human Frontier Science Program.

* To whom correspondence should be addressed: phone 33 4 38 78 31 19; fax 33 4 38 78 54 94; e-mail jean-michel.jault@ibs.fr.

‡ Institut de Biologie et Chimie des Protéines, UMR 5086 CNRS-Université de Lyon 1 and IFR 128 BioSciences Gerland-Lyon Sud.

§ Present address: Department of Chemistry, Purdue University, 560 Oval Dr., West Lafayette, IN 47907.

|| Institut Curie, UMR-CNRS 168.

⊥ Institut de Biologie Structurale, UMR 5075 Université Joseph Fourier/CEA/CNRS.

▽ Institut Curie, Unité INSERM 759.

£ McGill University.

[1] Abbreviations: ABC, ATP-Binding Cassette; NBD, Nucleotide-Binding Domain.

10.1021/bi702303s CCC: $40.75
Published on Web 01/24/2008

of MalK revealed no direct interaction between the two NBDs, which were nevertheless hold together by an additional specific C-terminal domain (*12*). This suggested that large conformational changes might take place during the catalytic cycle of ABC transporters, with the two NBDs engaging in, and disengaging from, a mutual interaction (*12*, *14*), and this is consistent with recent electron paramagnetic resonance (EPR) experiments performed on MsbA (*15*) or the 3D structures of MsbA obtained in four different conformations (*16*).

Identification of the step allowing substrate translocation in the catalytic cycle of ABC transporters is a fundamental question in order to understand how these transporters function. Both the ATP-induced NBD dimerization and ATP hydrolysis per se were suggested to provide an energy input sufficiently high to trigger substrate translocation (*9*, *17*−*19*). Here, we took advantage of the propensity of a multidrug ABC transporter from *Bacillus subtilis*, BmrA (formerly known as YvcC) (*20*), to form very peculiar, stable, ring-shaped structures in the absence of any effector (*21*) to study how nucleotide binding and/or hydrolysis might affect these structures. By use of mutants with either the putative catalytic base adjacent to the Walker B motif (E504) or the Walker A lysine (K380) substituted, and thereby blocked in different conformations of the ATPase cycle, it is shown that the ATP-dependent NBD dimerization of BmrA induces a conformational change large enough to either prevent formation of, or break, the rings. These observations are consistent with the ATP-induced dimerization of NBDs as being the "power stroke" of ABC transporters.

EXPERIMENTAL PROCEDURES

Unless specified, reagents were of the highest purity available and were purchased from Sigma. Dioleoylphosphatidylcholine (DOPC), dioleoylphosphatidylglycerol (DOPG), and nickel−nitrilotriacetic-1,2-dioleoyl-*sn*-glycero-3-{[*N*-(5-amino-1-carboxypentyl)iminodiacetic acid]succinyl} (Ni-NTA-DOGS) were of the highest purity available and were purchased from Avanti Polar Lipids. Dodecyl β-D-maltoside (DDM) was purchased from Anatrace.

Site-Directed Mutagenesis of BmrA. K380A and K380R mutants were constructed as previously described for the E504 mutants (*22*), with the oligonucleotides GCGTTCAAGCAGTTTAAACAGCGTCGTTGCTCCCCCGCCGCT and GCGTTCAAGCAGTTTAAACAGCGTCGTTCTTCCCCCGCCGCT, respectively, which introduce a new, silent, *Dra*I restriction site. Mutations were confirmed by DNA sequencing.

Purification and Reconstitution of BmrA Proteins. All mutant and wild-type proteins were purified and reconstituted into proteoliposomes according to the methods previously described (*22*).

ATPase Activity. The ATPase activity of BmrA reconstituted into proteoliposomes was monitored at 37 °C by ADP release coupled to the disappearance of reduced nicotinamide adenine dinucleotide (NADH) recorded at 340 nm. Measurements were performed in 50 mM Hepes [*N*-(2-hydroxyethyl)-piperazine-*N*′-ethanesulfonic acid]/KOH, pH 8, 4 mM phosphoenolpyruvate, pyruvate kinase (60 μg/mL), lactate dehydrogenase (32 μg/mL), and 0.3 mM NADH. Alternatively, when the sensitivity to vanadate inhibition was studied, ATPase activity was measured by a colorimetric assay of P_i release, as described previously (*23*).

Binding of 8-Azido-[α-^{32}*P*]*ATP.* Proteoliposomes containing either wild-type or mutant BmrA were incubated on ice for 5 min with increasing concentrations of 8-azido-[α-^{32}P]-ATP in a final volume of 50 μL of 50 mM Tris-HCl, pH 8, and 5 mM $MgCl_2$. After 5 min of UV irradiation (260 nm, UVS-II Minerallight), 200 μL of 50 mM Tris-HCl, pH 8, was added to the sample. An ultracentrifugation was then performed (400000*g*) for 30 min at 4 °C. Proteoliposomes were gently washed with 100 μL of ice-cold 50 mM Tris-HCl, pH 8, and pellets were resuspended in Laemmli buffer and submitted to electrophoresis. Gels were dried and submitted to autoradiography.

Vanadate or Beryllium Fluoride-Induced Trapping and Photoaffinity Labeling of Radioactive Nucleotides. Experiments were performed as previously described (*22*). $BeSO_4$ and NaF were prepared as water solutions and added separately to samples ($BeSO_4$ at the desired concentration and NaF in 5-fold excess).

Effects of Ligands on BmrA Ring-Shaped Structures. For reconstitution of ringlike structures, the purified proteins at 0.5 mg/mL were first supplemented with DDM (0.2% final concentration) and then with a mixture of egg phosphatidylcholine and egg phosphatidic acid (9/1 mol/mol) at a lipid-to-protein ratio of 1−1.6 (w/w), unless stated otherwise, and then supplemented with substrates as indicated. After 1 h of incubation at room temperature, the micellar solutions were treated with 40 mg of Bio-Beads/mL [ratio of BmrA/DDM/Bio-Beads was 0.5/2/40 (w/w/w)], according to a previously described procedure (*21*, *24*). Aliquots were taken at different time intervals for electron microscopic observations. Usually, the solution was withdrawn after 45 min of incubation with Bio-Beads, leading to a homogeneous preparation of ringlike structures that were stable for several days at 4 °C. Longer and complete detergent removal led to the formation of tubular membranes and vesicles. The reconstituted ring-shaped particles were then incubated with different ligands, as indicated, and analyzed by electron microscopy after 15−60 min incubation at room temperature. Samples were adsorbed onto carbon-coated 300 mesh copper grids and stained with 1% uranyl acetate.

Reconstitution of BmrA at the Air/Water Interface. Reconstitutions of wild-type and E504Q BmrA at the air/water interface were performed according to ref *25*. Briefly, proteins at 0.25 mg/mL in 50 mM Tris-HCl, pH 8, 5 mM $MgCl_2$, 150 mM KCl, 5 mM benzamidine, 50 mM imidazole, and 0.5% DDM were supplemented with dioleoylphosphocholine/dioleoylphosphatidylglycerol (9/1 mol/mol) at a lipid/protein ratio 0.5−1 (w/w) and solubilized for 4 h on ice. This mixture was injected with a 10-fold dilution below a lipid layer of Ni-NTA-DOGS and DOPC (1/1 ratio) previously spread at the air/water interface. The reconstitution well contained 60 μL of the binding solution: 50 mM Tris-HCl, pH 8, 5 mM $MgCl_2$, 150 mM KCl, 5 mM benzamidine, and 50 mM imidazole. After overnight binding of the His-tagged protein to the Ni^{2+}-lipid surface at 4 °C, detergent was removed by addition of 5 mg of Bio-Beads, leading to reconstitution after 2 days at 4 °C. Reconstitutions in the presence of nucleotides were performed as before with 5 mM ATP plus 1.5 mM orthovanadate (for the wild-type BmrA) or 5 mM ATP alone (for the E504Q mutant) in the

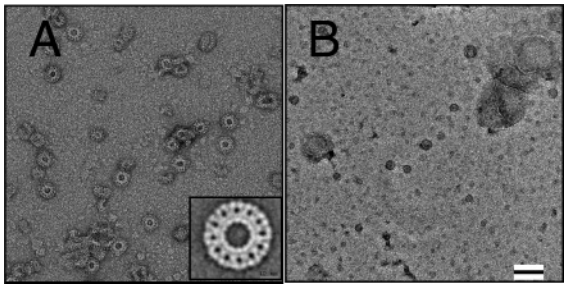

FIGURE 1: Electron microscopy of BmrA samples. (A) Negatively stained samples obtained after 45 min of progressive elimination of detergent from lipid−BmrA−detergent mixtures; stable ring-shaped structures of BmrA are observed. (B) The ring-shaped structures disappeared upon addition of ATP-Mg (7.5 mM each); scale bar corresponds to 50 nm. The inset in panel A corresponds to a projected top view of the cryoelectron microscopic 3D reconstruction of the BmrA ring-shaped structure, 40 nm in diameter, obtained as described earlier (*21*).

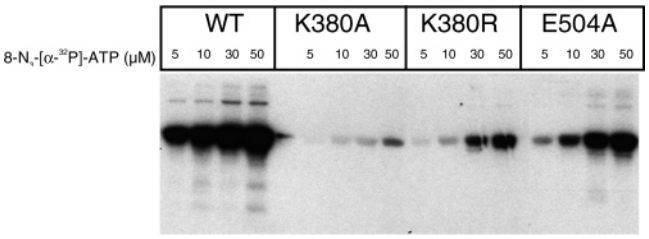

FIGURE 2: Binding of 8-azido-ATP to either wild-type or mutant BmrA. Increasing concentrations of 8-azido-[α-^{32}P]ATP, as indicated in the figure, were incubated at 4 °C for 5 min with either wild-type or mutant BmrA previously reconstituted into proteoliposomes. After 5 min of UV irradiation, samples were centrifuged, washed, and submitted to electrophoresis and autoradiography as described under Experimental Procedures.

reconstitution well. After reconstitution, the surfaces were picked up and stained with 2% uranyl acetate.

Electron Microscopy. Images were recorded in a low-dose mode on a Philips CM120 microscope operating at 120 kV at 800 nm defocus and a nominal magnification of 45000× by use of a 1024 × 1024 pixel Gatan charge-coupled device (CCD). The pixel size, as calibrated with bacteriorhodopsin 2D crystals, was 3.9 ± 0.1 Å.

RESULTS

We previously reported that BmrA formed very peculiar ring-shaped structures upon partial reconstitution at high protein/lipid ratios. The ring-shaped structures were made of 24 homodimers of BmrA embedded in a lipid bilayer and contained small amounts of detergent. These structures were remarkably stable over a wide range of experimental conditions, including various lipids and detergents, pH (from 6.0 to 9.0), salt concentration (from 50 to 500 mM NaCl), and temperature (from 4 to 37 °C) (*21*). Importantly, we show here that addition of both ATP and Mg^{2+}, in a concentration range (∼2−9 mM ATP) similar to that used to saturate wild-type BmrA during ATP hydrolysis (see ref *20* and also the caption to Figure 5), destroyed these ring-shaped structures, as illustrated on electron micrographs of negatively stained samples (Figure 1). Conversely, prior incubation with ATP and Mg^{2+} was able to prevent subsequent ring formation (not shown). Therefore, although these highly ordered structures were formed *in vitro*, this shows that the conformation of BmrA in these supramolecular structures is compatible with the binding of ATP-Mg and, thus, BmrA lies in a resting-state conformation suitable for its catalytic cycle. To substantiate this point, the ATPase activity of BmrA was studied before and after the formation of the rings (in the latter case, formation of the rings was first attested by visual inspection under the microscope). In 0.05% DDM, BmrA had an ATPase activity of ∼1.5 ± 0.24 μmol of ATP hydrolyzed min^{-1} mg^{-1}, a value comparable to that found previously under similar conditions (*26*), and this activity was sensitive to inhibition by 1 mM vanadate (∼0.17 ± 0.08 μmol of ATP hydrolyzed min^{-1} mg^{-1}). After formation of the rings, BmrA retained a high level of ATPase activity (1.35 ± 0.24 μmol of ATP hydrolyzed min^{-1} mg^{-1}) fully sensitive to vanadate inhibition (0.04 ± 0.08 μmol of ATP hydrolyzed min^{-1} mg^{-1}). Therefore, this gave us a unique opportunity to study conformational changes brought about by the binding of effectors on a whole ABC transporter embedded in a lipid bilayer environment and in a nativelike conformation. Various effectors were tested and, as shown in Table 1, disappearance of the rings was observed only when ATP (or a high concentration of the ATP analogue ATPγS) was used in the presence of Mg^{2+}. Other effectors tested, including ATP alone, Mg^{2+} alone, ADP plus Mg^{2+}, and vanadate (Table 1), or drug substrates such as 50 μM doxorubicin, did not induce destabilization of the rings. Because most of these effectors have been shown to bind both to the detergent-solubilized BmrA and to BmrA reconstituted into proteoliposomes (*20*), they probably also bind to BmrA in the lipid-containing ring-shaped structures. However, binding of these ligands does not seem to induce any detectable conformational rearrangement. In contrast, the binding of ATP-Mg or subsequent ATP hydrolysis triggers a conformational change large enough to destabilize the ring structure.

Table 1: Stability of the Rings in the Presence of Different Effectors

		effectors (mM)					
exp conditions[a]	*T* (°C)	ADP	ATPγS	ATP	Mg^{2+}	Vi	ring dissociation
1	**4**			**1.9**	**1.9**		+
1	4				1.9		−
2	23			60			−
2	**23**			**7.5**	**7.5**		+
2	23			7.5			−
2	23				7.5		−
2	23		4.5				−
2	23		4.5		4.5		−
3	23		12.5				−
3	**23**		**12.5**		**12.5**		+
3	23				12.5		−
3	23	10			10	5	−

[a] Rings were formed at 23 °C, in the presence of DDM as detergent and with egg phosphatidine choline/egg phosphatidine ethanolamine (9/1) and a lipid/protein ratio of 1.5, 1.6, or 1.1 (experimental conditions 1, 2, and 3, respectively). They were then incubated in the presence of different effectors, at either 4 or 23 °C, as indicated in the table. Boldface type highlights the conditions where the rings were destroyed (+); (−) indicates that the effectors had no effect on the performed rings.

In order to determine which step of BmrA ATPase cycle is responsible for this conformational change, we tested the capacity of several hydrolytically deficient mutants to alter the ring-shaped structure in the presence of ATP-Mg. The

Table 2: Ring Formation, or Dissociation, and ATPase Activities of Wild-Type or Mutant BmrA

		ring formation				ring dissociation			
proteins	ATPase activity[a]	control	Mg^{2+}	ATP	ATP/Mg^{2+}	control	Mg^{2+}	ATP	ATP/Mg^{2+}
wild-type	6500	+	+	+	−[b]	−	−	−	+[b]
K380A	0	+	+	+	+	−	−	−	−
K380R	150	+	+	+	+	−	−	−	−
E504A	0	+	+	+	−[b]	−	−	−	+[b]
E504Q	0	+	+	+	−[b]	−	nd[c]	nd	+[b]

[a] ATPase activities are expressed in nanomoles per minute per milligram of protein. When effectors were used, 7.5 mM was added. For ring formation, (+) indicates that formation of the rings was observed whereas (−) indicates that no rings were formed. For ring dissociation, (−) indicates that no effect was observed on the preformed rings, whereas (+) indicates that the rings were destroyed. [b] Conditions where no rings were observed, either directly in the presence of effectors (ring formation) or subsequent to the addition of effectors (ring dissociation). [c] Not determined.

first mutation studied concerned the E504 residue: the putative catalytic glutamate adjacent to the Walker B motif, in BmrA. We previously showed that its mutation to different residues totally abolished ATP hydrolysis by BmrA (*22*). We also chose to study two Walker A lysine mutants of BmrA, since this residue is known to be crucial for ATP hydrolysis in P-loop-containing ATPases (*27*−*29*). Besides, preliminary results obtained on K380 mutants of BmrA showed that whereas the K380A mutant was fully devoid of ATPase activity (Table 2), the K380R mutant retained a low but significant activity (∼2% that of the wild-type), which was insensitive to vanadate inhibition, in contrast to the wild-type BmrA. Despite this residual level of ATPase activity, the K380R mutant was nevertheless unable to transport either Hoechst 33342 (*20*) or doxorubicin (not shown). In order to characterize the catalytic step(s) altered in these mutants, their ability to bind nucleotides such as 8-azido-[α-^{32}P]ATP was assessed on ice (Figure 2). Although a significant loss in affinity and/or in photolabeling efficiency was observed in the K380 mutants as compared to either the wild-type or, to a lesser extent, the E504A mutant, this experiment clearly shows that the K380 mutants were still able to bind nucleotides. Trapping experiments were then performed to compare the properties of the E504A and K380R mutants. As previously observed, the E504A mutant trapped the 8-azido-[α-^{32}P]ATP tightly and in a vanadate-insensitive manner (Figure 3A), which was due to the total lack of ATPase activity, thereby leading to trapping of the ATP form of the analogue (*22*). In contrast, no significant labeling was observed for the K380R mutant under the same conditions, whether vanadate was present or not. A similar property was observed for Walker A lysine P-glycoprotein mutants (*30*, *31*), but importantly, some of them retained some trapping ability when BeF_x was used instead of vanadate (*32*). Therefore, we checked whether our K380 mutants could trap the 8-azido-[α-^{32}P]AT(D)P in the presence of BeF_x. As shown in Figure 3B, the K380A mutant was insensitive to BeF_x, in agreement with its lack of any detectable ATPase activity, whereas the K380R mutant was quite sensitive to this inhibitor and trapped much more 8-azido-[α-^{32}P]AT(D)P in the presence of 1 mM BeF_x than in its absence. The increase in trapping of the K380R mutant afforded by BeF_x was mainly due to accumulation of the 8-azido-[α-^{32}P]ADP, as evidenced from experiments using either α- or γ-labeled 8-azido-[^{32}P]ATP (Figure 3C), thus confirming that this mutant retains some residual hydrolytic ability.

We then tested the capacity of the different mutants to destabilize the ring-shaped structures of BmrA (Table 2). In the presence of ATP-Mg, both wild-type BmrA and the hydrolytically inactive E504 mutants either prevented ring formation or destroyed the preformed structures. Therefore, the conformational change responsible for the ring destabilization can be assigned to a prehydrolytic step of the catalytic cycle because the E504 mutants seem unable to perform even a single turnover (*22*). Further evidence for this hypothesis was provided by the reconstitution of wild-type BmrA and the E504Q mutant at the air/water interface. In these experiments, His-tagged proteins were first bound to a lipid ligand bearing a Ni-nitrilotriacetic acid head group and then reconstituted into a lipid bilayer at a high protein/lipid ratio (Figure 4). Compared to the classical reconstitution in bulk, where the proteins have no initial constraints for their assembly, here they are bound to the planar lipidic surface during the reconstitution process. Previous reconstitution of different types of membrane proteins by this method had always led to planar membranes (*25*), except for P-glycoprotein, where tubular vesicles have been reported (*33*). It was found here that, in the absence of any substrate and after binding and reconstitution of BmrA upon detergent removal, both the wild-type BmrA and the E504Q mutant formed tubular-shaped membranes, and the tubular structures have a diameter of ∼40 nm with a variable length (0.3−1 μM, Figure 4A,C). This unexpected 3D organization was likely dictated by the shape of the proteins, thereby inducing a high membrane curvature. When wild-type BmrA was reconstituted in the presence of ATP-Mg alone, some 2D crystals were observed on the grid but the majority of the membrane remained in a tubular shape, suggesting that the protein adopted different conformations (not shown). In contrast, in the presence of both ATP-Mg and vanadate, which led to the trapping of wild-type BmrA in a transition-state conformation, only planar membranes with some 2D crystalline arrays were obtained (Figure 4B). For the E504Q mutant, planar membranes were obtained whether or not vanadate was included together with ATP-Mg (see Figure 4D for the condition in the absence of vanadate), showing that the binding of ATP-Mg alone is sufficient to reach a stable conformation. On the other hand, for the K380 mutants, we have been unable so far to obtain 2D crystals regardless of the conditions used.

By sharp contrast with the glutamate mutants, the K380 mutants appeared unable to operate any substantial conformational change upon ATP-Mg binding because, in the presence of these ligands, the lysine mutants still formed the rings, and preformed rings were not dissociated after ATP-Mg addition (Table 2). Therefore, we surmised that, in contrast to the E504 mutants, the K380 ones might lack

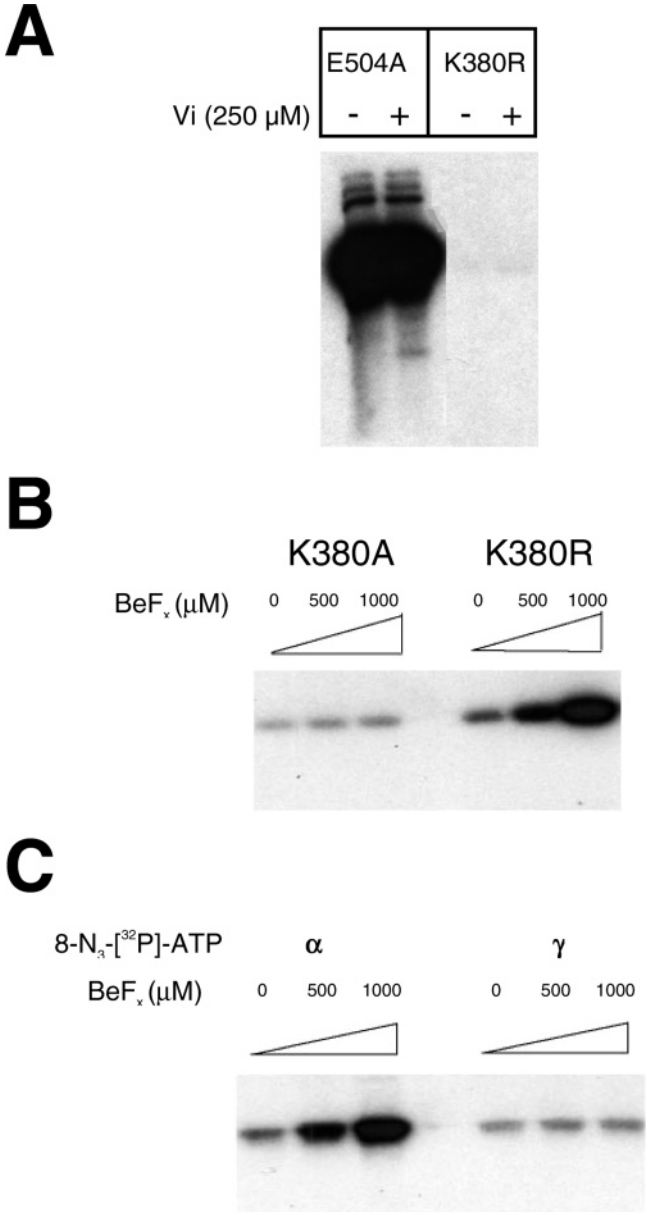

FIGURE 3: Trapping of 8-azido-ATP by BmrA mutants. Proteoliposomes containing 3 μg of BmrA mutants were incubated with 8-azido-[α or γ-^{32}P]ATP (0.25−0.35 Ci/mmol) in 50 mM Tris-HCl, pH 8, and 3 mM $MgCl_2$, with or without either 250 μM vanadate or the indicated concentrations of BeF_x, in a total volume of 50 μL at 37 °C for 10 min. Incubations were stopped by transferring the tubes on ice and by adding 1 mM cold ATP. Free and loosely bound labeled nucleotides were removed by centrifugation at 400000*g* for 30 min at 4 °C. Proteoliposomes were then gently washed with 100 μL of ice-cold 50 mM Tris-HCl, pH 8, and pellets were resuspended in 15 μL of the same buffer, kept on ice, and irradiated with UV light for 5 min. Laemmli buffer was then added to the samples, and after 20 min of mixing, samples were resolved by electrophoresis. Gels were dried and submitted to autoradiography. (A) Vanadate (Vi) trapping of 5 μM 8-azido-[α-^{32}P]ATP by E504A and K380R mutants. (B) Beryllium fluoride-induced 8-azido-[α-^{32}P]ATP (50 μM) trapping by K380 mutants. (C) Beryllium fluoride-induced 8-azido-ADP trapping in the K380R mutant; experiments were performed with 50 μM either 8-azido-[α-^{32}P]ATP or 8-azido-[γ-^{32}P]ATP.

the capacity to dimerize via their NBDs. To test this hypothesis, we studied the ATPase activity of the K380R mutant as a function of ATP-Mg concentration, because we had shown previously that wild-type BmrA displayed positive cooperativity for ATP hydrolysis (*20*). In contrast to wild-type BmrA, the K380R mutant hydrolyzed ATP according to Michaelis−Menten kinetics (Figure 5), suggesting that its ATPase activity is catalyzed independently by each NBD. Therefore, it is conceivable that the ATP-driven dimerization step of NBDs is impaired in the two K380 BmrA mutants, thus preventing destabilization of the BmrA ring structures.

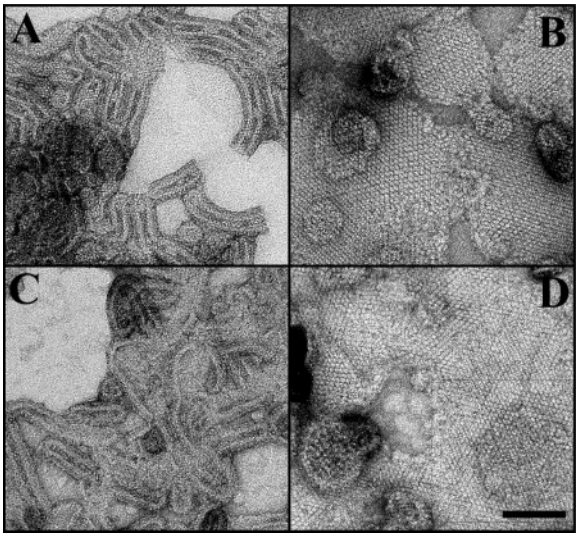

FIGURE 4: Reconstitution of BmrA at the air/water interface. His-tagged proteins solubilized in micelles of lipids and detergents were bound to a Ni^{2+}-lipid at the air/water interface. Upon complete detergent removal, proteins were incorporated into a lipid bilayer in which they can form 2D crystalline arrays. After reconstitution, the surfaces were picked up, negatively stained, and analyzed by electron microscopy. Reconstitution of wild-type BmrA in the absence (A) and in the presence (B) of Mg-ATP plus vanadate and reconstitution of E504Q mutant in the absence (C) and in the presence (D) of Mg-ATP is shown. Note the change of morphology from tubular (A, C) to planar membranes (B, D). Bar: 50 nm.

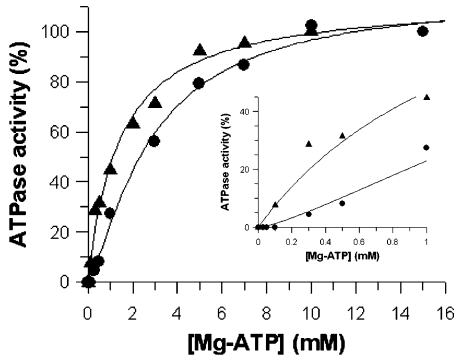

FIGURE 5: ATPase activity of wild-type (●) or K380R BmrA mutant (▲) as a function of Mg-ATP concentration. ATPase activity was expressed as the percentage of maximal activity. Maximum (100%) activity corresponds to 6.5 or 0.15 μmol ATP hydrolyzed min^{-1} (mg of protein)$^{-1}$ for wild-type or K380R BmrA mutant, respectively. (Inset) ATPase activity of the two variants at low Mg-ATP concentrations. Curve fittings were performed with SigmaPlot 8.0 (SPSS Inc.), and the values obtained for the best fits were as follows: for wild-type BmrA, Hill number = 1.33 ± 0.14 and $K_{m\ app}$ = 2.83 mM ± 0.37, and for the mutant, which did not show any positive cooperativity, a Michaelis−Menten fitting gave K_m = 1.42 mM ± 0.19.

DISCUSSION

Different pieces of evidence suggest that the molecular mechanism of ABC transporters involves substantial conformational changes, especially those triggered by ATP-Mg

binding and/or hydrolysis (*15*, *16*, *34*, *35*; for a recent review, see ref *36*), and a similar scenario is likely to occur for BmrA (*37*). ATP-driven dimerization of NBDs and their dissociation upon ATP hydrolysis are thought to propagate conformational changes in the transmembrane domains (TMDs) that are associated with substrate transport (*8*, *17*, *36*, *38*). Importantly, 2D crystals of P-glycoprotein showed that AMP-PNP binding to the transporter caused a major repacking of TMDs and a reduction in drug-binding affinity (*39*). However, the recent structure of a new putative ABC importer showed an inward-facing conformation (*40*), in contrast to the outward-facing conformation of BtuCD (*13*), although both of them were resolved in nucleotide-free states. As suggested by the authors, the energetic basis of the differential stabilization of alternate conformations is not obvious and might be due to the substitution of the native bilayer with detergent, shifting the equilibrium between the two conformations in absence of their ligands (*40*). Moreover, the 3D structure of the drugs exporter Sav1866, containing either ADP-Mg or AMP-PNP, showed a similar closed conformation for the two NBDs (*41*, *42*). The authors suggested the possibility that the purification and crystallization conditions, particularly the presence of detergent, could have shifted the conformational equilibrium of Sav1866 toward the ATP-bound state when ADP-Mg was present (*41*). In our present study, the ring-shaped structures, in which BmrA is embedded, provide a highly stable lipid environment suitable to study conformational changes associated with the catalytic cycle of this transporter.

As shown for different ABC transporters, ATP-Mg first binds to separate, noninteracting NBDs to initiate the ATPase cycle (*43*−*47*). For the purified multidrug P-glycoprotein, this first step occurs with low affinity [$K_d \sim 0.5$ mM (*48*)], probably on separate NBDs, and this is consistent with the low affinity found for isolated recombinant NBDs (*49*, *50*). The two Walker A BmrA mutants described here are still able to bind both ATP-Mg and the 8-N_3-ATP nucleotide analogue, albeit with a seemingly reduced efficiency, and this is in agreement with the results found after mutation of the equivalent Lys residue in other ABC transporters (*30*, *38*, *51*−*53*). Mounting evidence supports the view that, in all native ABC transporters, the ATP-Mg binding step triggers the dimerization of the two NBDs in a transient conformation where two ATP molecules are tightly sandwiched at the NBDs interface (*9*, *12*, *45*, *47*, *54*−*56*). While this certainly holds true for wild-type BmrA, our data suggest that this ATP-Mg dependent dimerization step is impaired in the Walker A mutants (see Figure 6), for the following reasons: (i) In contrast to wild-type BmrA, the K380R mutant hydrolyzes ATP according to Michaelis−Menten kinetics. (ii) This lack of cooperativity is not simply due to the very low ATPase activity of the K380R mutant because it also shows an unusual insensitivity to vanadate inhibition. Likewise, the 8-N_3-ATP trapping abilities of both Walker A mutants were insensitive to the presence of vanadate, as previously reported when the equivalent lysine residue of P-glycoprotein was mutated (*30*, *31*). The lack of positive cooperativity together with a lack of sensitivity to vanadate inhibition of the ATPase activity have been previously reported for some isolated wild-type NBDs (*57*, *58*), which probably reflects a lack of proper interaction between the two NBDs. Indeed, it has been shown that the tight

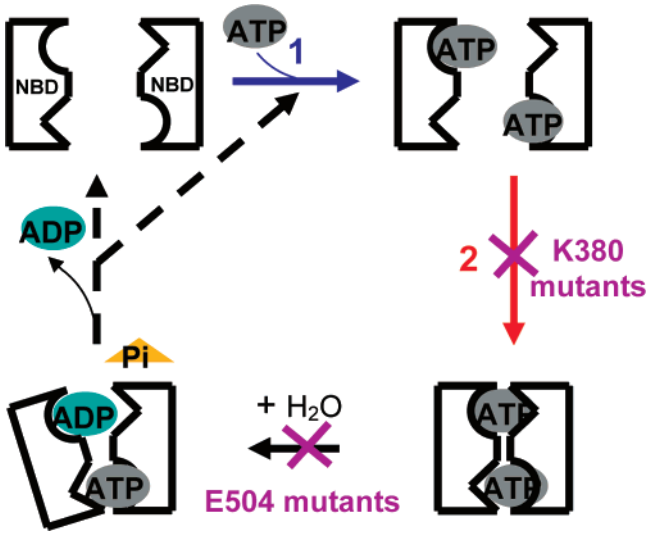

FIGURE 6: Schematic drawing of the minimal ATPase cycle of BmrA. In the resting state, BmrA is in an open conformation, where the two NBDs do not interact and thus lie far apart from each other. To engage the catalytic cycle, ATP-Mg binds to each NBD (step 1). This induces a tight dimerization of the two NBDs (step 2). In the normal catalytic cycle of wild-type BmrA, ATP hydrolysis and products release (ADP + P_i) dissociate the NBDs, and BmrA returns to its resting state (i.e., an open conformation). The steps impaired in the two sets of mutants, E504 and K380, are indicated. As both wild-type transporter and hydrolysis-inactive E504 mutants destabilize the rings, step 2 is proposed to be responsible for the ring dissociation (i.e., the hydrolysis of ATP is not required to destroy the ring).

dimerization of the NBDs is required to reach the vanadate-sensitive state in P-glycoprotein (*59*), which is quite consistent with the vanadate-catalyzed photocleavage in the S signature of the opposite NBD in the maltose transporter (*7*). (iii) Further support for the contention of a deficient ATP-Mg-dependent dimerization step in our BmrA mutants came from the study of the Atm1p half-transporter, where mutation of the equivalent lysine residue has been shown to prevent efficient dimerization (*60*). Interestingly, mutation of the equivalent lysine in one of the two NBDs of P-glycoprotein also abolished the hydrolytic capacity of the nonmutated NBD (*30*), a result that might be explained by the inability of the mutant transporter to efficiently dimerize during the catalytic cycle. On the other hand, whereas a GlcV homodimer bearing either the E166A or G144A mutation was totally inactive, a mixture of both mutants produced an active heterodimer, suggesting that disruption of one active site could be tolerated if the dimer could still be formed (*61*), and similar observations were also reported with HisP and HlyB (*56*, *62*). (iv) Finally, whereas the K380A mutant was insensitive to BeF_x, in agreement with its complete lack of ATPase activity, the K380R mutant was sensitive to this inhibitor (Figure 3B), which allowed the trapping of 8-N_3-ADP (Figure 3C). Consistent with this, it has been shown, by use of BeF_x instead of Vi, that some Walker A lysine mutants of P-glycoprotein still retain some residual hydrolytic activity (*32*). Interestingly, a recent study on ABCG5/ABCG8 heterodimer reported that ABCG5 alone was able to trap 8-N_3-ADP in the presence of BeF_x, showing that hydrolysis may occur on this half-size subunit in the absence of the partner ABCG8 subunit (*52*). Importantly, it has been shown that the inhibitory state trapped by BeF_x was clearly different from that reached in the presence of Vi (*63*, *64*). This result

was consistent with the 3D structure of myosin in complex with MgADP·Vi, which revealed an expected conformation mimicking the transition state (*65*), whereas a rather prehydrolytic state resembling the ATP-Mg-induced conformation was found in the presence of MgADP·BeF_x (*66*).

The properties exhibited by the E504 BmrA mutants are clearly different from those found for the K380 mutants (Figure 3A). Previous characterization had shown that, upon Mg-8-N_3-ATP binding, the E504 mutants underwent a conformational change, driving the trapping of azido-ATP into one of the two NBDs (*22*), a conclusion consistent with that drawn from equivalent mutations in P-glycoprotein (*67*−*69*). Because mutations of the equivalent glutamate residue have been reported to form quite stable NBD dimers in the presence of ATP (*45*, *54*), it seems reasonable to assume that binding of ATP to each NBD in E504 mutants triggers the tight dimerization of the two NBDs (Figure 6). However, it is important to note here that if a subsequent step of washing was included, only one of the two ATP molecules (or ATP-γ-S) previously occluded remained tightly bound at the NBD interface of either BmrA or P-glycoprotein (*22*, *69*, *70*).

On the basis of both the lack of detectable ATPase activity in the E504 mutants and their propensity to trap only the 8-N_3-ATP form of the analogue (not the ADP derivative) (*22*), we had previously proposed that the glutamate residue might constitute the catalytic base of ABC transporters (*5*, *22*). Although this residue is clearly essential to sustain a high level of ATPase activity, its mutation in some ABC transporters still allowed some residual ATPase activity (*10*, *45*, *68*, *71*, *72*). In contrast, mutation of the conserved histidine residue to an alanine, within the so-called H-loop of ABC transporters, totally abolished the ATPase activity of the recombinant NBD from HlyB, leading to the suggestion of a substrate-assisted catalysis rather than an acid−base mechanism for ATP hydrolysis (*10*). Regardless of the chemical mechanism used by ABC transporters, we have also mutated the equivalent histidine to alanine in BmrA, and the purified protein still showed some residual ATPase activity (∼50 nmol of ATP hydrolyzed min^{-1} mg^{-1}), therefore precluding the use of this mutant here to prevent ATP hydrolysis. It is therefore conceivable that, depending on the ABC transporter studied, mutation of the equivalent glutamate residue differentially affects the ATPase activity, hence leading to a totally inactive enzyme for BmrA and LolD (*22*, *54*) while leaving a residual activity for other ABC transporters including HlyB (*10*). On the other hand, in the presence of ATP-Mg alone, the E504Q mutant could reach a quite stable conformation permitting the growth of 2D crystals, whereas the wild-type BmrA required both ATP-Mg and Vi to stabilize a conformation compatible with crystal growth. The stable ATP-Mg conformation reached by the E504 mutants is consistent with its lack of ATPase activity previously reported and agrees well with the 3D crystal obtained for the equivalent mutation in the LolD enzyme (*9*). Therefore, we propose that the different behavior observed for the two types of mutants, E504 and K380, regarding the ring formation/dissociation reflects their different capacity to dimerize. Both types of mutant are able to bind ATP to a noninteracting NBD (Figure 6, step 1). Once ATP is bound, this will trigger the dimerization of the two NBDs (Figure 6, step 2), but only in the case of either E504 mutants or the wild-type enzyme. For K380 mutants, this step is impaired and the two NBDs will not engage in formation of a tight NBD dimer. As a consequence, rings remain stable and insensitive to ATP-Mg addition. For the K380R mutant, ATP bound to a single NBD will eventually be hydrolyzed, thus allowing a very sluggish ATPase activity. How the mutations of the Walker A lysine alter the tight dimerization of the two NBDs is currently unknown. It has been shown that this process requires a perfect orientation of the ABC signature of one subunit onto the nucleotide bound to the opposite NBD (*9*, *11*, *12*). This requires a rotation of the helical subdomain of the NBD with respect to the ATP-binding subdomain of the same NBD [intramolecular rotation (*11*, *73*, *74*)], and possibly such a conformational rotation is prevented by the mutation introduced here. Regarding the E504 mutants, because they are unable to hydrolyze ATP, they remain trapped in the conformation where ATP is sandwiched at the NBD interface of the tight dimer (Figure 6, step 2). Therefore, we propose that this tight NBD dimerization step is responsible for the ring destruction.

In conclusion, the minimal scheme proposed here for the ATPase cycle of BmrA is based on both biochemical and low-resolution structural information, and it is compatible with that proposed for P-glycoprotein by Senior's group (*69*). ATP-driven dimerization of the two NBDs is believed to be one of the most energetic steps of the catalytic cycle of ABC transporters (*9*, *17*, *19*), and here we bring some evidence that this step induces a conformational change in BmrA sufficiently large to destabilize the suprastructure of the rings. In contrast, a low level of ATP hydrolysis does not seem to alter the ring structure if the dimerization process is impaired (i.e., if hydrolysis of ATP takes place on a single noninteracting NBD). Relevant to this, the K380R mutant was shown previously to be unable to catalyze drug transport (*20*), and our results argue that this is due to a lack of NBD dimerization, thereby leading to a slow, uncoupled ATPase activity. Overall, our results support the proposal that the ATP-driven dimerization of NBDs in ABC transporters is able to propagate large conformational changes in transmembrane domains, possibly coupled to substrate translocation.

ACKNOWLEDGMENT

We thank Dr. Olivier Dalmas for critical reading of the manuscript.

REFERENCES

1. Saier, M. H., Jr. (2000) A functional-phylogenetic classification system for transmembrane solute transporters, *Microbiol. Mol. Biol. Rev. 64*, 354−411.
2. Holland, I. B., and Blight, M. A. (1999) ABC-ATPases, adaptable energy generators fuelling transmembrane movement of a variety of molecules in organisms from bacteria to humans, *J. Mol. Biol. 293*, 381−399.
3. Higgins, C. F. (2001) ABC transporters: physiology, structure and mechanism—an overview, *Res. Microbiol. 152*, 205−210.
4. Borst, P., and Elferink, R. O. (2002) Mammalian ABC transporters in health and disease, *Annu. Rev. Biochem. 71*, 537−592.
5. Geourjon, C., Orelle, C., Steinfels, E., Blanchet, C., Deleage, G., Di Pietro, A., and Jault, J. M. (2001) A common mechanism for ATP hydrolysis in ABC transporter and helicase superfamilies, *Trends Biochem. Sci. 26*, 539−544.
6. Davidson, A. L., and Chen, J. (2004) ATP-binding cassette transporters in bacteria, *Annu. Rev. Biochem. 73*, 241−268.

7. Fetsch, E. E., and Davidson, A. L. (2002) Vanadate-catalyzed photocleavage of the signature motif of an ATP-binding cassette (ABC) transporter, *Proc. Natl. Acad. Sci. U.S.A. 99*, 9685−9690.
8. Jones, P. M., and George, A. M. (2004) The ABC transporter structure and mechanism: perspectives on recent research, *Cell. Mol. Life Sci. 61*, 682−699.
9. Smith, P. C., Karpowich, N., Millen, L., Moody, J. E., Rosen, J., Thomas, P. J., and Hunt, J. F. (2002) ATP binding to the motor domain from an ABC transporter drives formation of a nucleotide sandwich dimer, *Mol. Cell 10*, 139−149.
10. Zaitseva, J., Jenewein, S., Jumpertz, T., Holland, I. B., and Schmitt, L. (2005) H662 is the linchpin of ATP hydrolysis in the nucleotide-binding domain of the ABC transporter HlyB, *EMBO J. 24*, 1901−1910.
11. Zaitseva, J., Oswald, C., Jumpertz, T., Jenewein, S., Wiedenmann, A., Holland, I. B., and Schmitt, L. (2006) A structural analysis of asymmetry required for catalytic activity of an ABC-ATPase domain dimer, *EMBO J. 25*, 3432−3443.
12. Chen, J., Lu, G., Lin, J., Davidson, A. L., and Quiocho, F. A. (2003) A tweezers-like motion of the ATP-binding cassette dimer in an ABC transport cycle, *Mol. Cell 12*, 651−661.
13. Locher, K. P., Lee, A. T., and Rees, D. C. (2002) The *E. coli* BtuCD structure: a framework for ABC transporter architecture and mechanism, *Science 296*, 1091−1098.
14. Hanekop, N., Zaitseva, J., Jenewein, S., Holland, I. B., and Schmitt, L. (2006) Molecular insights into the mechanism of ATP-hydrolysis by the NBD of the ABC-transporter HlyB, *FEBS Lett. 580*, 1036−1041.
15. Borbat, P. P., Surendhran, K., Bortolus, M., Zou, P., Freed, J. H., and McHaourab, H. S. (2007) Conformational motion of the ABC transporter MsbA induced by ATP hydrolysis, *PLoS Biol. 5*, e271.
16. Ward, A., Reyes, C. L., Yu, J., Roth, C. B., and Chang, G. (2007) Flexibility in the ABC transporter MsbA: Alternating access with a twist, *Proc. Natl. Acad. Sci. U.S.A. 104*, 19005−19010.
17. Higgins, C. F., and Linton, K. J. (2004) The ATP switch model for ABC transporters, *Nat. Struct. Mol. Biol. 11*, 918−926.
18. Ambudkar, S. V., Kim, I. W., and Sauna, Z. E. (2006) The power of the pump: mechanisms of action of P-glycoprotein (ABCB1), *Eur. J. Pharm. Sci. 27*, 392−400.
19. Austermuhle, M. I., Hall, J. A., Klug, C. S., and Davidson, A. L. (2004) Maltose-binding protein is open in the catalytic transition state for ATP hydrolysis during maltose transport, *J. Biol. Chem. 279*, 28243−28250.
20. Steinfels, E., Orelle, C., Fantino, J. R., Dalmas, O., Rigaud, J. L., Denizot, F., Di Pietro, A., and Jault, J. M. (2004) Characterization of YvcC (BmrA), a Multidrug ABC Transporter Constitutively Expressed in *Bacillus subtilis*, *Biochemistry 43*, 7491−7502.
21. Chami, M., Steinfels, E., Orelle, C., Jault, J. M., Di Pietro, A., Rigaud, J. L., and Marco, S. (2002) Three-dimensional structure by cryo-electron microscopy of YvcC, an homodimeric ATP-binding cassette transporter from *Bacillus subtilis*, *J. Mol. Biol. 315*, 1075−1085.
22. Orelle, C., Dalmas, O., Gros, P., Di Pietro, A., and Jault, J. M. (2003) The conserved glutamate residue adjacent to the Walker-B motif is the catalytic base for ATP hydrolysis in the ATP-binding cassette transporter BmrA, *J. Biol. Chem. 278*, 47002−47008.
23. Steinfels, E., Orelle, C., Dalmas, O., Penin, F., Miroux, B., Di Pietro, A., and Jault, J. M. (2002) Highly efficient over-production in *E. coli* of YvcC, a multidrug-like ATP-binding cassette transporter from *Bacillus subtilis*, *Biochim. Biophys. Acta 1565*, 1−5.
24. Rigaud, J. L., Mosser, G., Lacapere, J. J., Olofsson, A., Levy, D., and Ranck, J. L. (1997) Bio-Beads: an efficient strategy for two-dimensional crystallization of membrane proteins, *J. Struct. Biol. 118*, 226−235.
25. Levy, D., Chami, M., and Rigaud, J. L. (2001) Two-dimensional crystallization of membrane proteins: the lipid layer strategy, *FEBS Lett. 504*, 187−193.
26. Ravaud, S., Do Cao, M. A., Jidenko, M., Ebel, C., Le Maire, M., Jault, J. M., Di Pietro, A., Haser, R., and Aghajari, N. (2006) The ABC transporter BmrA from Bacillus subtilis is a functional dimer when in a detergent-solubilized state, *Biochem. J. 395*, 345−353.
27. Senior, A. E., Wilke-Mounts, S., and al-Shawi, M. K. (1993) Lysine 155 in beta-subunit is a catalytic residue of *Escherichia coli* F1 ATPase, *J. Biol. Chem. 268*, 6989−6994.
28. Smith, C. A., and Rayment, I. (1996) Active site comparisons highlight structural similarities between myosin and other P-loop proteins, *Biophys. J. 70*, 1590−1602.
29. Schneider, E., and Hunke, S. (1998) ATP-binding-cassette (ABC) transport systems: functional and structural aspects of the ATP-hydrolyzing subunits/domains, *FEMS Microbiol. Rev. 22*, 1−20.
30. Urbatsch, I. L., Beaudet, L., Carrier, I., and Gros, P. (1998) Mutations in either nucleotide-binding site of P-glycoprotein (Mdr3) prevent vanadate trapping of nucleotide at both sites, *Biochemistry 37*, 4592−4602.
31. Urbatsch, I. L., Julien, M., Carrier, I., Rousseau, M. E., Cayrol, R., and Gros, P. (2000) Mutational analysis of conserved carboxylate residues in the nucleotide binding sites of P-glycoprotein, *Biochemistry 39*, 14138−14149.
32. Szakacs, G., Ozvegy, C., Bakos, E., Sarkadi, B., and Varadi, A. (2000) Transition-state formation in ATPase-negative mutants of human MDR1 protein, *Biochem. Biophys. Res. Commun. 276*, 1314−1319.
33. Lee, J. Y., Urbatsch, I. L., Senior, A. E., and Wilkens, S. (2002) Projection structure of P-glycoprotein by electron microscopy. Evidence for a closed conformation of the nucleotide binding domains, *J. Biol. Chem. 277*, 40125−40131.
34. Vigano, C., Julien, M., Carrier, I., Gros, P., and Ruysschaert, J. M. (2002) Structural and functional asymmetry of the nucleotide-binding domains of P-glycoprotein investigated by attenuated total reflection Fourier transform infrared spectroscopy, *J. Biol. Chem. 277*, 5008−5016.
35. Rosenberg, M. F., Callaghan, R., Modok, S., Higgins, C. F., and Ford, R. C. (2005) Three-dimensional structure of P-glycoprotein: the transmembrane regions adopt an asymmetric configuration in the nucleotide-bound state, *J. Biol. Chem. 280*, 2857−2862.
36. Callaghan, R., Ford, R. C., and Kerr, I. D. (2006) The translocation mechanism of P-glycoprotein, *FEBS Lett. 580*, 1056−1063.
37. Dalmas, O., Orelle, C., Foucher, A. E., Geourjon, C., Crouzy, S., Di Pietro, A., and Jault, J. M. (2005) The Q-loop disengages from the first intracellular loop during the catalytic cycle of the multidrug ABC transporter BmrA, *J. Biol. Chem. 280*, 36857−36864.
38. Gadsby, D. C., Vergani, P., and Csanady, L. (2006) The ABC protein turned chloride channel whose failure causes cystic fibrosis, *Nature 440*, 477−483.
39. Rosenberg, M. F., Velarde, G., Ford, R. C., Martin, C., Berridge, G., Kerr, I. D., Callaghan, R., Schmidlin, A., Wooding, C., Linton, K. J., and Higgins, C. F. (2001) Repacking of the transmembrane domains of P-glycoprotein during the transport ATPase cycle, *EMBO J. 20*, 5615−5625.
40. Pinkett, H. W., Lee, A. T., Lum, P., Locher, K. P., and Rees, D. C. (2007) An inward-facing conformation of a putative metal-chelate-type ABC transporter, *Science 315*, 373−377.
41. Dawson, R. J., and Locher, K. P. (2006) Structure of a bacterial multidrug ABC transporter, *Nature 443*, 180−185.
42. Dawson, R. J., and Locher, K. P. (2007) Structure of the multidrug ABC transporter Sav1866 from *Staphylococcus aureus* in complex with AMP-PNP, *FEBS Lett. 581*, 935−938.
43. Muller, K. M., Ebensperger, C., and Tampe, R. (1994) Nucleotide binding to the hydrophilic C-terminal domain of the transporter associated with antigen processing (TAP), *J. Biol. Chem. 269*, 14032−14037.
44. Berridge, G., Walker, J. A., Callaghan, R., and Kerr, I. D. (2003) The nucleotide-binding domains of P-glycoprotein. Functional symmetry in the isolated domain demonstrated by *N*-ethylmaleimide labelling, *Eur. J. Biochem. 270*, 1483−1492.
45. Janas, E., Hofacker, M., Chen, M., Gompf, S., van der Does, C., and Tampe, R. (2003) The ATP hydrolysis cycle of the nucleotide-binding domain of the mitochondrial ATP-binding cassette transporter Mdl1p, *J. Biol. Chem. 278*, 26862−26869.
46. Ramaen, O., Sizun, C., Pamlard, O., Jacquet, E., and Lallemand, J. Y. (2005) Attempts to characterize the NBD heterodimer of MRP1: transient complex formation involves Gly771 of the ABC signature sequence but does not enhance the intrinsic ATPase activity, *Biochem. J. 391*, 481−490.
47. Pretz, M. G., Albers, S. V., Schuurman-Wolters, G., Tampe, R., Driessen, A. J., and van der Does, C. (2006) Thermodynamics of the ATPase cycle of GlcV, the nucleotide-binding domain of the glucose ABC transporter of *Sulfolobus solfataricus*, *Biochemistry 45*, 15056−15067.
48. Liu, R., and Sharom, F. J. (1996) Site-directed fluorescence labeling of P-glycoprotein on cysteine residues in the nucleotide binding domains, *Biochemistry 35*, 11865−11873.
49. Baubichon-Cortay, H., Baggetto, L. G., Dayan, G., and Di Pietro, A. (1994) Overexpression and purification of the carboxyl-terminal

nucleotide-binding domain from mouse P-glycoprotein. Strategic location of a tryptophan residue, *J. Biol. Chem. 269*, 22983−22989.
50. Dayan, G., Baubichon-Cortay, H., Jault, J. M., Cortay, J. C., Deleage, G., and Di Pietro, A. (1996) Recombinant N-terminal nucleotide-binding domain from mouse P-glycoprotein. Overexpression, purification, and role of cysteine 430, *J. Biol. Chem. 271*, 11652−11658.
51. Muller, M., Bakos, E., Welker, E., Varadi, A., Germann, U. A., Gottesman, M. M., Morse, B. S., Roninson, I. B., and Sarkadi, B. (1996) Altered drug-stimulated ATPase activity in mutants of the human multidrug resistance protein, *J. Biol. Chem. 271*, 1877−1883.
52. Zhang, D. W., Graf, G. A., Gerard, R. D., Cohen, J. C., and Hobbs, H. H. (2006) Functional asymmetry of nucleotide-binding domains in ABCG5 and ABCG8, *J. Biol. Chem. 281*, 4507−4516.
53. Berger, A. L., Ikuma, M., and Welsh, M. J. (2005) Normal gating of CFTR requires ATP binding to both nucleotide-binding domains and hydrolysis at the second nucleotide-binding domain, *Proc. Natl. Acad. Sci. U.S.A. 102*, 455−460.
54. Moody, J. E., Millen, L., Binns, D., Hunt, J. F., and Thomas, P. J. (2002) Cooperative, ATP-dependent association of the nucleotide binding cassettes during the catalytic cycle of ATP-binding cassette transporters, *J. Biol. Chem. 277*, 21111−21114.
55. Vergani, P., Lockless, S. W., Nairn, A. C., and Gadsby, D. C. (2005) CFTR channel opening by ATP-driven tight dimerization of its nucleotide-binding domains, *Nature 433*, 876−880.
56. Zaitseva, J., Jenewein, S., Wiedenmann, A., Benabdelhak, H., Holland, I. B., and Schmitt, L. (2005) Functional characterization and ATP-induced dimerization of the isolated ABC-domain of the haemolysin B transporter, *Biochemistry 44*, 9680−9690.
57. Nikaido, K., Liu, P. Q., and Ames, G. F. (1997) Purification and characterization of HisP, the ATP-binding subunit of a traffic ATPase (ABC transporter), the histidine permease of *Salmonella typhimurium*. Solubility, dimerization, and ATPase activity, *J. Biol. Chem. 272*, 27745−27752.
58. Greller, G., Horlacher, R., DiRuggiero, J., and Boos, W. (1999) Molecular and biochemical analysis of MalK, the ATP-hydrolyzing subunit of the trehalose/maltose transport system of the hyperthermophilic archaeon *Thermococcus litoralis*, *J. Biol. Chem. 274*, 20259−20264.
59. Urbatsch, I. L., Tyndall, G. A., Tombline, G., and Senior, A. E. (2003) P-glycoprotein catalytic mechanism: studies of the ADP-vanadate inhibited state, *J. Biol. Chem. 278*, 23171−23179.
60. Chloupkova, M., Reaves, S. K., LeBard, L. M., and Koeller, D. M. (2004) The mitochondrial ABC transporter Atm1p functions as a homodimer, *FEBS Lett. 569*, 65−69.
61. Verdon, G., Albers, S. V., van Oosterwijk, N., Dijkstra, B. W., Driessen, A. J., and Thunnissen, A. M. (2003) Formation of the productive ATP-Mg^{2+}-bound dimer of GlcV, an ABC-ATPase from *Sulfolobus solfataricus*, *J. Mol. Biol. 334*, 255−267.
62. Nikaido, K., and Ames, G. F. (1999) One intact ATP-binding subunit is sufficient to support ATP hydrolysis and translocation in an ABC transporter, the histidine permease, *J. Biol. Chem. 274*, 26727−26735.
63. Sankaran, B., Bhagat, S., and Senior, A. E. (1997) Inhibition of P-glycoprotein ATPase activity by beryllium fluoride, *Biochemistry 36*, 6847−6853.
64. Russell, P. L., and Sharom, F. J. (2006) Conformational and functional characterization of trapped complexes of the P-glycoprotein multidrug transporter, *Biochem. J. 399*, 315−323.
65. Smith, C. A., and Rayment, I. (1996) X-ray structure of the magnesium(II)·ADP·vanadate complex of the *Dictyostelium discoideum* myosin motor domain to 1.9 Å resolution, *Biochemistry 35*, 5404−5417.
66. Fisher, A. J., Smith, C. A., Thoden, J. B., Smith, R., Sutoh, K., Holden, H. M., and Rayment, I. (1995) X-ray structures of the myosin motor domain of *Dictyostelium discoideum* complexed with MgADP·BeF_x and MgADP·AlF_4, *Biochemistry 34*, 8960−8972.
67. Tombline, G., Bartholomew, L. A., Tyndall, G. A., Gimi, K., Urbatsch, I. L., and Senior, A. E. (2004) Properties of P-glycoprotein with mutations in the "catalytic carboxylate" glutamate residues, *J. Biol. Chem. 279*, 46518−46526.
68. Tombline, G., Bartholomew, L. A., Urbatsch, I. L., and Senior, A. E. (2004) Combined mutation of catalytic glutamate residues in the two nucleotide binding domains of P-glycoprotein generates a conformation that binds ATP and ADP tightly, *J. Biol. Chem. 279*, 31212−31220.
69. Tombline, G., Muharemagic, A., White, L. B., and Senior, A. E. (2005) Involvement of the "occluded nucleotide conformation" of P-glycoprotein in the catalytic pathway, *Biochemistry 44*, 12879−12886.
70. Sauna, Z. E., Kim, I. W., Nandigama, K., Kopp, S., Chiba, P., and Ambudkar, S. V. (2007) Catalytic cycle of ATP hydrolysis by P-glycoprotein: Evidence for formation of the E·S reaction intermediate with ATP-γ-S, a nonhydrolyzable analogue of ATP, *Biochemistry 46*, 13787−13799.
71. Sauna, Z. E., Muller, M., Peng, X. H., and Ambudkar, S. V. (2002) Importance of the conserved Walker B glutamate residues, 556 and 1201, for the completion of the catalytic cycle of ATP hydrolysis by human P-glycoprotein (ABCB1), *Biochemistry 41*, 13989−14000.
72. Carrier, I., Julien, M., and Gros, P. (2003) Analysis of catalytic carboxylate mutants E552Q and E1197Q suggests asymmetric ATP hydrolysis by the two nucleotide-binding domains of P-glycoprotein, *Biochemistry 42*, 12875−12885.
73. Lu, G., Westbrooks, J. M., Davidson, A. L., and Chen, J. (2005) ATP hydrolysis is required to reset the ATP-binding cassette dimer into the resting-state conformation, *Proc. Natl. Acad. Sci. U.S.A. 102*, 17969−17974.
74. Yuan, Y. R., Blecker, S., Martsinkevich, O., Millen, L., Thomas, P. J., and Hunt, J. F. (2001) The crystal structure of the MJ0796 ATP-binding cassette. Implications for the structural consequences of ATP hydrolysis in the active site of an ABC transporter, *J. Biol. Chem. 276*, 32313−32321.

BI702303S